Weak Lensing Results from GEMS

**Catherine Heymans[1]†, Michael L. Brown[2], Marco Barden[1],
John A. R. Caldwell[3], Knud Jahnke[4], Hans-Walter Rix[1],
Andy N. Taylor[2], Steve Beckwith[3], Eric Bell[1], Andrea Borch[1],
Boris Häußler[1], Sharda Jogee[3], Daniel H. McIntosh[5],
Klaus Meisenheimer[1], Chen Peng[6], Sebastian F. Sánchez[4],
Rachel Somerville[3], Lutz Wisotzki[4] and Christian Wolf[7]**

[1]Max-Plank-Institut für Astronomie, Königsthul 17, 69115 Heidelberg, Germany.

[2]Institute for Astronomy, University of Edinburgh, Blackford Hill, Edinburgh, EH9 3HJ, UK.

[3] Space Telescope Science Institute, 3700 San Martin Drive, Baltimore MD, 21218, USA.

[4]Astrophysikalisches Institut Potsdam, An der Stenwarte 16, 14482 Potsdam, Germany.

[5] University of Massachusetts, 710 North Pleasant Street, Amherst, MA 01003, USA.

[6]Steward Observatory, University of Arizona, 933 N. Cherry Ave., Tuscon AZ, 85721, USA.

[7] Department of Astrophysics, University of Oxford, Keble Road, Oxford, OX1 3RH, UK.

Abstract. We present our cosmic shear analysis of the Galaxy Evolution from Morphology and SEDs (GEMS) survey. Imaged with the Advanced Camera for Surveys (ACS) on HST, GEMS provides high resolution imaging spanning some 800 square arcmins in the Chandra Deep Field South (CDFS). We discuss the benefits of using space-based data for weak lensing studies and show that the ACS is a very powerful instrument in this regard. We find that we are not limited by systematic errors arising from the anisotropic ACS point spread function distortion and use our cosmic shear results to place joint constraints on the matter density parameter Ω_m and the amplitude of the matter power spectrum σ_8, finding $\sigma_8(\Omega_m/0.3)^{0.62} = 0.73 \pm 0.12$.

To investigate the impact of atmospheric seeing on weak lensing analysis we compare the shear measured from CDFS galaxies resolved by the COMBO-17 survey and imaged by GEMS. We find good agreement between the two surveys and a higher dispersion in the intrinsic ellipticity distribution of COMBO-17. This dispersion implies that a space-based cosmic shear analysis would yield higher signal-to-noise results compared to a ground-based cosmic shear analysis of the same galaxy sample.

1. Introduction

Weak gravitational lensing by large scale structure shears images of background galaxies, inducing weak correlations in the observed ellipticities of galaxies. The amplitude and angular dependence of these correlations are directly related to the non-linear matter power spectrum $P_\delta(k)$ and the geometry of the Universe (see Bartelmann & Schneider (2001) and references within). Following the success of the first generation of cosmic shear surveys, where joint constraints were placed on the matter density parameter Ω_m and the amplitude of the matter power spectrum σ_8, several ground based surveys are currently underway that will image of the order of a hundred square degrees, providing exquisite data sets for future weak lensing analysis. These surveys will however be subject to atmospheric seeing which erases the weak lensing shear information from all galaxies smaller than the size of the seeing disk. This, in effect, limits the maximum depth of ground based weak lensing surveys and hence their ultimate sensitivity, leading to proposals for future

† email: heymans@mpia.de

deep wide-field space-based observations (see the contribution from Alexandre Refregier in these proceedings).

With the installation of the Advanced Camera for Surveys (ACS) on HST, relatively wide-field space-based weak lensing studies are now feasible and in this conference proceeding we present constraints on Ω_m and σ_8 from our detection of weak gravitational lensing by large scale structure in the Galaxy Evolution from Morphology and SEDs survey (GEMS).

2. The GEMS survey

The GEMS survey spans an area of 28.2×28.2 arcmins centred on the Chandra Deep Field South (CDFS), combining 125 orbits of ACS/HST time with supplementary data from the GOODS project (Giavalisco *et al.* (2004)). See Rix *et al.* (2004) for an overview of the GEMS survey. The full mosaic has been imaged in both the F606W and F850LP passbands from which we use the deeper F606W data for our cosmic shear analysis. Sources are identified using the *SExtractor* software yielding a catalogue of 65 resolved galaxies per square arcmin detected above the 15σ level.

The accuracy of any weak lensing analysis depends critically on the correction for the distorting point spread function (PSF) of the telescope and camera, characterised through images of stellar objects. As a result of the wide field of view of the ACS, the relative stability of the ACS PSF over time, and the observing strategy of GEMS, whereby 95% of the data was imaged in the space of 20 days, the PSF of the ACS during the GEMS observations is well characterised.
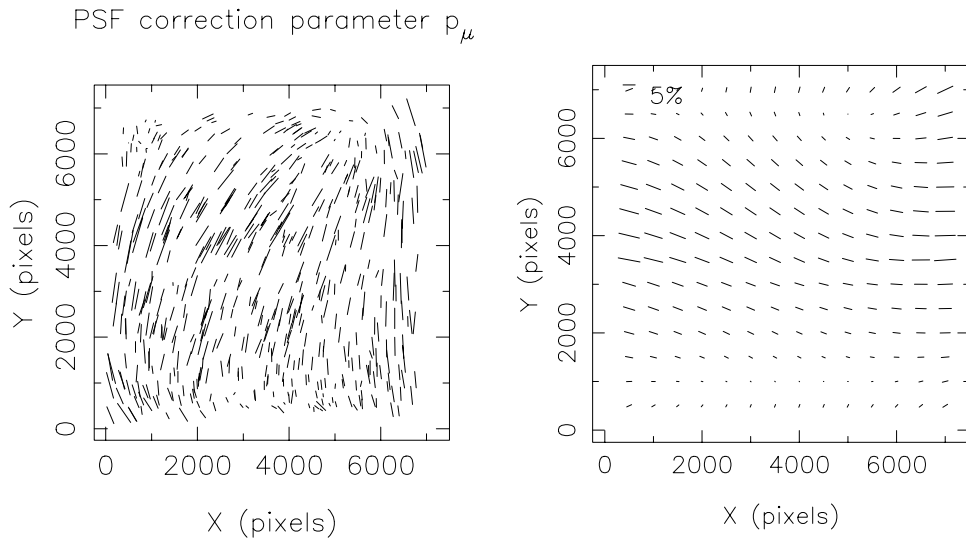
Figure 1. Left: The variation across the ACS field of view of the measured PSF correction vector $p(r_g)$ with r_g set equal to the mean galaxy size of 5.9 pixels. Right: Comparing the two-dimensional polynomial models of p measured from the first and last half of the GEMS observations reveals PSF variation that is at a maximum level of $\Delta\varepsilon^* = 5\%$.

We use the method of Kaiser, Squires & Broadhurst (1995), Luppino & Kaiser (1997) and Hoekstra *et al.* (1998) (KSB+) to invert the effects of the PSF smearing and shearing in order to recover an unbiased estimate of galaxy shear γ. The left panel of figure 1 shows the variation across the ACS field of view of the measured KSB+ PSF correction vector

p where

$$p_\mu(r_g) = (P^{\mathrm{sm}*})^{-1}_{\mu\alpha}(r_g)\,\varepsilon_\alpha^{*\,\mathrm{obs}}(r_g). \tag{2.1}$$

P^{sm} is the smear polarizability tensor given in Hoekstra *et al.* (1998) and $\varepsilon^{*\,\mathrm{obs}}$ is the observed weighted stellar ellipticity, where r_g defines the width of the Gaussian weight function. Owing to the non-Gaussian nature of the ACS PSF p changes as a function of scale size r_g and we therefore create models $p(r_g)$. Figure 1 clearly reveals the anisotropy of the PSF distortion which is at the level of $\sim 5\,\%$. We model $p(r_g)$ with a two-dimensional second order polynomial for the first and second half of the GEMS observations, assuming PSF stability on the scale of 10 days. These models are then used to correct galaxy ellipticities for PSF distortion following KSB+. Note that for the GOODS images which comprise the central 15 ACS tiles of the GEMS mosaic, we characterise a third set of PSF models using all stars imaged by GOODS, as the different dithering patterns of GOODS and GEMS impacts on the PSF.

The right panel of figure 1 shows the difference between the stellar ellipticity predicted by the two GEMS PSF models. These models, calculated from the first and second half of the GEMS observations, reveal variation in the ACS PSF which, at maximum, is at the level of $\Delta\epsilon^* \sim 5\,\%$. PSF time variation in space-based instruments can result from telescope 'breathing', as the HST goes into and out of sunlight in its 90 minute orbit, and from a slow change in focus which is periodically corrected for (Rhodes, Refregier & Groth (2000)). Variation in the PSF as measured from reduced data will also be caused by differences in data reduction methods, although with GEMS the consistent observation and reduction strategy will help to minimise this effect. It is currently unclear where the variation in the GEMS PSF arises, but it is clear that within the duration of the GEMS observations the PSF variation is small. We find that the correlation between stellar and galaxy ellipticity is consistent with zero, as shown in figure 2, and therefore conclude that the semi-time dependent PSF modelling that we have applied in this analysis copes adequately with small instabilities in the ACS PSF.
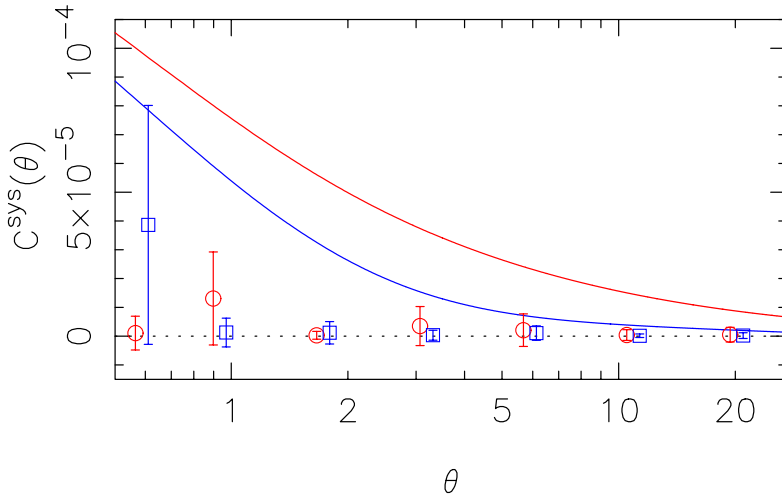
Figure 2. Star-galaxy cross correlation functions $C_{tt}^{\mathrm{sys}} = \langle\gamma_t\varepsilon_t^*\rangle^2/\langle\varepsilon_t^*\varepsilon_t^*\rangle$ (circles) and $C_{rr}^{\mathrm{sys}} = \langle\gamma_r\varepsilon_r^*\rangle/\langle^2\varepsilon_r^*\varepsilon_r^*\rangle$ (squares) compared to theoretical galaxy-galaxy shear correlation functions $\langle\gamma_t\gamma_t\rangle$ (upper curve) and $\langle\gamma_r\gamma_r\rangle$ (lower curve) with $\Omega_m = 0.3$, and $\sigma_8 = 0.75$. We find that the star-galaxy cross correlation is consistent with zero indicating that the measurement of galaxy-galaxy shear correlations from the GEMS data will be free from major sources of systematics.

3. Analysis

We measure the mean shear correlation function $\langle \gamma_{t_r} \gamma_{t_r} \rangle_\theta$ and full statistical covariance matrix from the GEMS data using a modified jackknife method. With knowledge of the survey redshift distribution, the shear correlation function can be directly related to the non-linear mass power spectrum P_δ, where the exact relationship can be found in Bartelmann & Schneider (2001). We estimate the median redshift z_m of the GEMS survey based on redshifts from the COMBO-17 survey (Wolf *et al.* (2004)) and VVDS survey (Le Fèvre *et al.* (2004)) finding $z_m = 0.95 \pm 0.1$.
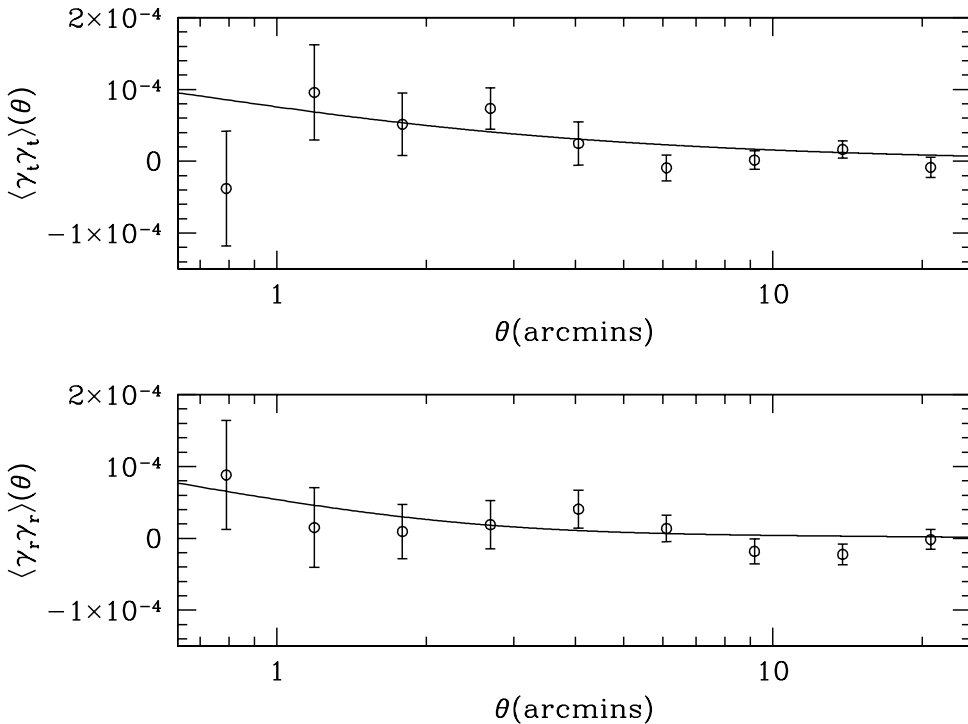
Figure 3. Shear correlation functions $\langle \gamma_t \gamma_t \rangle_\theta$ (upper) $\langle \gamma_r \gamma_r \rangle_\theta$ (lower) estimated from GEMS using a modified jackknife technique. Over-plotted is the best fit theoretical model with $\Omega_m = 0.3$, and $\sigma_8 = 0.73$

Figure 3 shows our jackknife estimate of the shear correlation functions with the best fit theoretical model over-plotted. Assuming a flat cosmology $\Omega_m + \Omega_\Lambda = 1$ and marginalising over the Hubble constant H_0, with a Gaussian prior set by the WMAP results with $H_0 = 72 \pm 5 \, \mathrm{km \, s^{-1} \, Mpc^{-1}}$ (Spergel *et al.* (2003)) we place joint constraints on σ_8 and Ω_m such that

$$\sigma_8 (\Omega_m/0.3)^{0.62} = 0.73 \pm 0.12, \tag{3.1}$$

where the likelihood surface is shown in figure 4. We note that these error bars do not include the uncertainty arising from sample variance. The CFDS is a factor of two under-dense in massive galaxies (Wolf *et al.* (2003)) and we might therefore expect a relatively low measurement of σ_8 from this field.
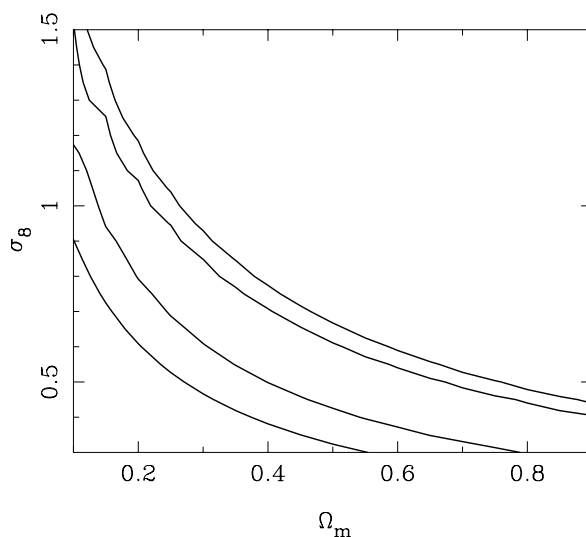
Figure 4. The likelihood surface of σ_8 and Ω_m as measured from the GEMS shear correlation function. The inner and outer contours correspond to 1 and 2σ confidence regions.

4. Comparison with COMBO-17 ground based data

It is interesting to note that cosmological parameters constraints from GEMS are very similar to those from the COMBO-17 survey (Brown *et al.* (2003)) a deep multi-colour survey which spans ~ 5 times the area of GEMS. This results from the higher number density of resolved galaxies in space-based data and the higher signal-to-noise measurements of galaxy shear which are achievable with higher resolution data.

The deep R band COMBO-17 data in the CDFS allows us to directly compare galaxy shear measurement from atmosphere limited data with high resolution space-based data. Figure 5 compares galaxy shear measured for a subsample of GEMS galaxies that are resolved in the 0.8 arcsec seeing deep R-band COMBO-17 data. The individual galaxy shear measurements from both surveys are, on average, in fairly good agreement with noticeably larger dispersion in the intrinsic ellipticity distribution measured by COMBO-17. This increased dispersion implies that a space-based cosmic shear analysis would yield higher signal-to-noise results compared to a ground-based cosmic shear analysis of the same galaxy sample.

The slight offset between the two surveys hints at a potential calibration bias related to the Luppino & Kaiser (1997) correction for atmospheric seeing and quadrupole weighting. Using sheared image simulations it will be possible to resolve this issue.

5. Conclusions

We have detected weak lensing by large scale structure in the GEMS survey, setting joint constraints on the matter density parameter Ω_m and the amplitude of the matter power spectrum, σ_8. This result demonstrates the power of the ACS on HST for weak lensing studies.

The comparison of space-based GEMS data and ground-based COMBO-17 data has shown that galaxy shear is measured to a higher accuracy from space-based data. This evidence, combined with the fact that the increased number density of resolved galaxies
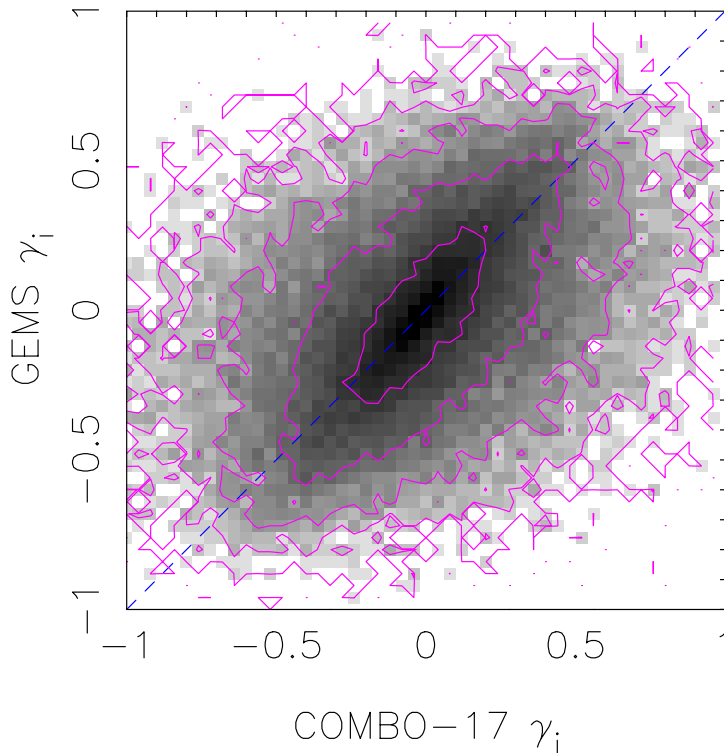
Figure 5. Comparison of individual galaxy shear measurements from GEMS space-based data and COMBO-17 ground-based data for a subsample of GEMS galaxies that are resolved in COMBO-17 imaging. There is fairly good agreement between the two surveys with a larger intrinsic ellipticity dispersion in the COMBO-17 measurement.

from space-based data allows one to probe the power spectrum to redshifts $z > 1$, strongly supports the drive towards future large wide-field imaging surveys from space.

A more detailed description of the GEMS weak lensing analysis can be found in Heymans $et\ al.$ (in prep), and the comparison of space-based and ground-based data can be found in Brown $et\ al.$ (in prep).

References

Bartelmann, M. & Schneider, P. 2001, Physics Reports, 340, 291

Brown, M.L., Taylor, A.N., Bacon, D., Gray, M., Dye, S., Meisenheimer, K. & Wolf, C. 2003, MNRAS, 341, 100

Giavalisco, M. $et\ al.$ 2004, ApJL, 600, L93

Hoekstra, H., Franx, M., Kuijken, K. & Squires,G. 1998, ApJ, 504, 636

Kaiser, N., Squires, G. & Broadhurst, T. 1995, ApJ, 449, 460

Le Fèvre, O. $et\ al.$ 2004, A&A submitted

Luppino, G. & Kaiser, N. 1995, ApJ, 475, 20

Rhodes, J., Refregier, A. & Groth, E. 2000, ApJ, 536, 79

Rix, H-W. $et\ al.$ 2004, ApJ Suppl.152, 163.

Spergel, D. $et\ al.$ 2003, ApJ Suppl., 148, 175

Wolf, C., Meisenheimer, K., Rix, H-W., Borch, A., Dye, S. & Kleinheinrich, M. 2003, A&A, 401, 73

Wolf, C. $et\ al.$ 2004, A&A, 421, 913